Crop Classification with Multi-Temporal Satellite Imagery

Rose M. Rustowicz,
roserust@stanford.edu

Figure 1: The two datasets, Scene 1 and 2, used for the project. Each example is a temporal signature of a pixel scene location throughout an agricultural growing season (time). The output are predictions for each agricultural crop type in the scene.

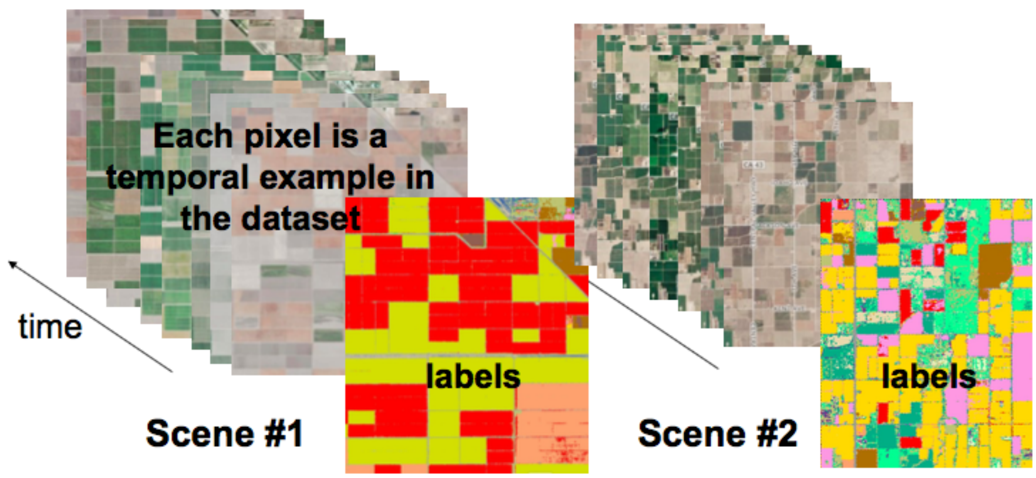

1 Introduction and Related Work

In this report, I explore the use of time series satellite imagery and machine learning for crop classification. Crop classification is important for understanding the agricultural cover of our evermore populated planet. Remote sensing data, such as calibrated imagery from satellites, can be helpful in monitoring food growth across the globe. Studies via satellite imagery are often limited to public data with low revisit rates and/or coarse spatial resolution. However, a recent surge in satellite data from new-aerospace companies provide daily imagery with relatively high spatial resolution. High revisit rates in satellite image capture enable the incorporation of temporal information into crop classification schemes. With high cadence temporal information just now becoming available, there is plenty of room to explore the data and methods for classification.

Land Cover Classification Land cover, as the name describes, refers to land surface types such as vegetation, rock, road, water, etc. Land cover classification studies attempt to predict labels of surface classes, where in the case of this paper, we use supervised machine learning techniques. Many land cover classification methods use mono-temporal information from only one glimpse in time. In most of these cases, features for classification are extracted from spectral and texture properties of the surfaces. However, for some land cover classes, such as crops, *Foerster et. al.* [1] show that land cover properties change over time, where different crop types have unique growth cycles throughout the year. This emphasizes our hypothesis that incorporation of temporal data into the classification scheme will aid in producing successful crop classification.

Machine Learning Machine learning describes algorithms that learn from data rather than being explicitly programmed. With a rise in data and computational abilities over the last decade, the field has gained tremendous popularity. In regards to crop classification, there has been previous work that uses machine learning [2 - 4], although it is much less common to incorporate temporal information into the classification scheme, as in [5]. In this report, we continue to explore machine learning algorithms for crop classification, with use of temporal crop information. We explore the supervised machine learning methods of multi-class logistic regression (also referred to as softmax regression), support vector machines (SVMs), a simple neural network (NN), and a convolutional neural network (CNN). The input examples to our models are one-dimensional temporal signatures of spectral values for pixel locations throughout a scene. The models predict probabilities for each of the crop types.

2 Dataset Construction

With no current standard for temporal crop classification datasets, two separate datasets were constructed. Satellite data of crop fields was taken from the Planet Explorer API [6], and labels were constructed from the USDA Crop Data Layer database [7]. The USDA Crop Data Layer provides annual crop maps throughout the United States at 30 meter spatial resolution per pixel, while the Rapid Eye data from Planet has 5 meter spatial resolution per pixel. Both sources were cropped to the same area of interest (AOI) defined by latitude and longitude coordinates, and the USDA data was sampled to match the Rapid Eye pixel resolution. The most recent USDA layer available is from the 2016 growing season. Because crop fields are rotated from year to year, we must use the Planet data collected from the same year.

We use the Planet Explorer API to search for Rapid Eye data within a specified AOI that has minimal cloud cover (< 5 %), maximum overlap (> 99 % with the AOI), and falls in a date range from February 1, 2016 to December 31, 2016. Each Rapid Eye image has five spectral bands that represent blue, green, red, red edge, and near infrared spectral values. We get valid images at fifteen time stamps over two scenes, with at least one image per month. Scene 1 is a simpler dataset with six crop types, while Scene 2 is a more complicated, sporadic dataset with nine crop types, see Figure 1. To define the pixels that will make up the datasets, we mask the top six and nine crops, respectively, from the USDA data, and only consider the pixels that fall under these masks (see masks in Figure 2). Scene 1 contains crop classes of cotton, safflower, tomato, winter wheat, durum wheat, and idle land in about 35 million pixels. Scene 2 contains crop classes of alfalfa, almonds, corn, cotton, idle land, pistachios, walnuts, winter wheat, and a corn/winter wheat mix in about 20 million pixels. To balance the datasets, we randomly select 100,000 pixels from each crop and add it to the corresponding dataset. We shuffle the selected examples and use a 90-05-05 split for the training, validation, and test sets, respectively. For Scene 1, this leaves us with a training set of 540,000 examples, a validation set of 30,000 examples, and a test set of 30,000 examples, where each example (a pixel location in space) has 75 features (15 time stamps of 5 spectral bands). Scene 2 contains nine crop types, with a training set of 810,000 examples, a validation set of 45,000 examples, and a test set of 45,000 examples.

To compare the multi-temporal results to a mono-temporal case, we select one time stamp from each scene in mid-July. This scene image has five total features, which are the values in the 5 spectral bands measurements, at only one time stamp.

Figure 2: The left six masks show crop classes in Scene 1: In clockwise order are cotton, safflower, tomato, idle crop land, durum wheat, and winter wheat. Masks of each crop class in Scene 2 are shown in the right nine masks: In clockwise order are alfalfa, almonds, corn, cotton, corn/winter wheat, winter wheat,walnuts, pistachios, and idle land.

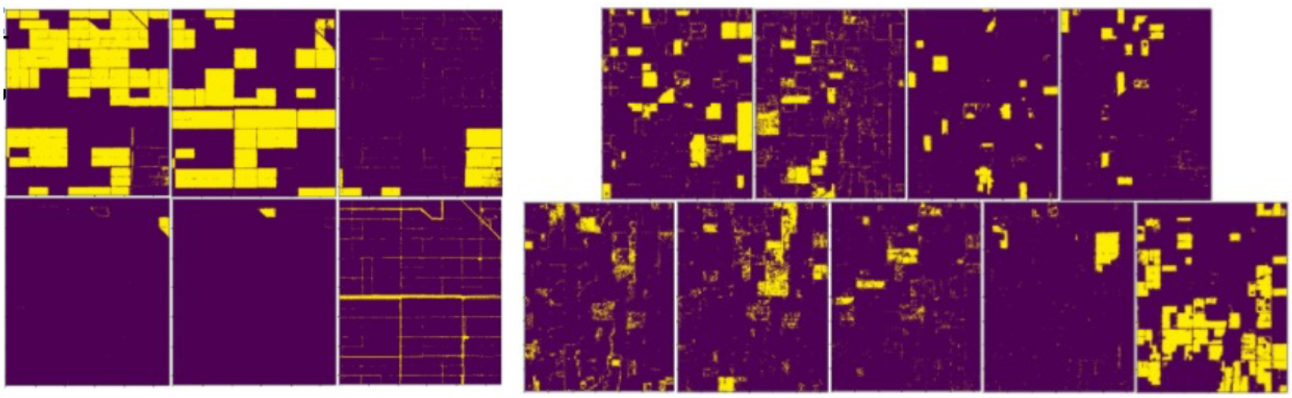

3 Methods

We explored a variety of supervised machine learning methods, including softmax regression, support vector machines (SVMs), a one-layer neural network (NN), and a convolutional neural network (CNN).

3.1 Softmax Regression

Softmax regression is an extension of logistic regression for multi-class classification. In the multi-class case, the hypothesis function estimates the probability of $p(y = i|x; \theta)$ as

$$h_{\theta_i}(x) = \frac{\exp(\theta_i^T x)}{\sum_{j=1}^{k-1} \exp(\theta_i^T x)}, \forall i = 1, ..., k-1$$

where k is the number of output predictions. The hypothesis function is defined in $k-1$ dimensions, where the last dimension $p(y = k|x; \theta) = 1 - \sum_{i=1}^{k-1} h_{\theta_i}(x)$. To obtain an objective function, we take the log likelihood of $p(y = i|x; \theta)$:

$$l(\theta) = \sum_{i=1}^{m} \log p(y^{(i)}|x^{(i)}; \theta) = \sum_{i=1}^{m} \log \prod_{l=1}^{k} \left(\frac{\exp(\theta_l^T x^1)}{\sum_{j=1}^{k} \exp(\theta_j^T x^{(i)})}\right)^{1 y^{(i)}=l}$$

The log-likelihood function can then be maximized by running gradient descent or another optimization method with respect to the parameters θ.

In our approach, we used sklearn's logistic regression function [8] to implement softmax regression. The most successful performance on the validation sets minimized the multinomial loss (compared to the 'one vs. rest' approach, which fits a binary loss for each label). We use l2 regularization, and find the best results with a regularization value of 0.1.

3.2 Support Vector Machines

SVMs separate classes by finding a hyperplane that maximizes the margins between class support vectors. When classes are not linearly separable, kernels can be used to find the hyperplane that best separates the data in a higher dimensional space. Simply put, SVMs minimize a regularized cost function with hinge loss.

Hinge loss is defined as: $L(z, y) = max(0, 1 - yz)$. The goal of SVMs is to find $\overline{w} \in \mathbb{R}^n$ and $b \in \mathbb{R}$ that minimize

$$J(\overline{w}, b) = \Sigma_{i=1}^{m} L(\overline{w}x^{(i)} - b, y^{(i)}) + \frac{\lambda}{2}||\overline{w}||^2$$

We use sklearn's SVM functions [9] to implement the SVM classifier. The most successful performance on the validation sets used a RBF kernel with a small regularization value, $\lambda =$ 1e-6, and a gamma value of 0.1, which is used in the sklearn implementation to specify the importance of each individual example. As gamma was increased, the training score increased, while validation score decreased. This indicates that a large value of gamma leads to over fitting. As regularization weight decreased, validation score increased. In this case, increasing the regularization weight does not seem to help the model, but rather hurt it. The SVM models were trained on a smaller training set of 60,000 examples to produce these results. The validation and test sets remained the same.

3.3 Simple Neural Network (NN)

At a high level, NNs mimic neural connections inspired by the human brain. As long as the path of each mathematical connection is differentiable, the weights of the network can be learned through backpropagation. We implement a simple one-layer neural network with the Keras sequential modeling framework [10]. The model has a hidden layer with 200 neurons, uses a rectified linear unit (relu) activation function for the hidden layer and a softmax activation function at the output, cross entropy loss, a dropout rate of 0.1, and a regularization strength of $\lambda =$ 1e-5. Adadelta [11], a technique that uses an adaptive learning rate, is used to optimize for the model parameters. The Xavier initialization method [12] is used to initialize weights, and biases are initialized to zero. We train for 100 epochs with a batch size of 1000 examples. The same number of hidden units and output predictions are used in the mono-temporal case, except that the model input only has five features, and so the model is also retrained for this case.

3.4 Convolutional Neural Network (CNN)

A CNN shares connection weights in each layer, rather than in the NN where each neuron has a unique connection to every other neuron in neighboring layers. Backpropagation is also used to find the network parameters, stored in matrices of convolutional kernels. CNNs are known for performing well in recognition tasks, and so we apply them here to identify features in the temporal crop signatures. The CNN architecture used is shown is Figure 3.

For the multi-temporal model, the convolutional layers in the network have 32 and 64 neurons, respectively, while the fully-connected layer has 1000 neurons. For the mono-temporal model, the convolutional layers have 8 and 16 neurons, respectively, while fully-connected layer has 200 neurons. The model was simplified to give better performance for the lower-dimensional input feature space of the mono-temporal inputs. Weights were initialized with the Xavier initialization method, a cross entropy loss was used, and the network parameters were optimized with the Adam optimizer [13]. In all cases, training ran for 10 epochs, with a batch size of 100 examples.

Figure 3: The CNN architecture used for the project. Each example is a temporal signature, which is why the network input are vectors rather than matrices.

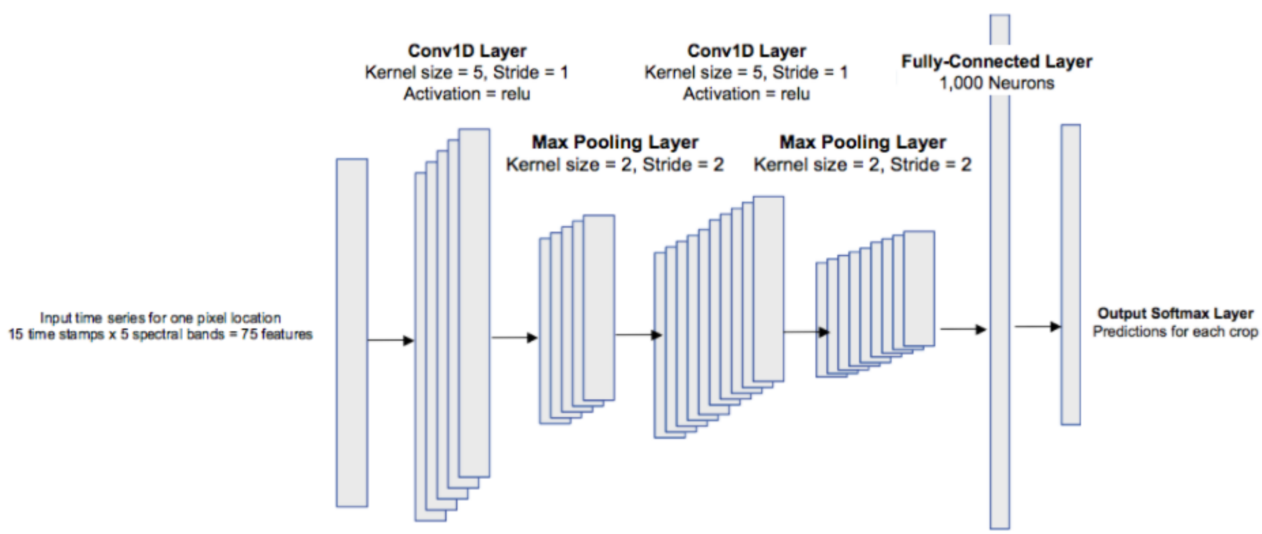

4 Results

Quantitative results for each of the supervised learning methods are outlined in Tables 1 - 4. Tables 1 and 3 show the results of the multi-temporal models for Scene 1 and Scene 2, respectively. Tables 2 and 4 show the results of the mono-temporal models for Scene 1 and Scene 2, respectively. A comparison between scenes indicates that all models had higher prediction accuracies on the simpler scene (Scene 1), as expected. Results for Scene 2, the more complicated scene, show improved prediction accuracy as the models become more complicated, going from left to right in table columns. A comparison between multi-temporal and mono-temporal results shows an increase in performance from added temporal information. This provides an important insight that temporal information is helpful for crop classification, showing that crops have distinguishable temporal signatures throughout the growing season.

Table 1: Scene 1 Multi-Temporal Results

	Softmax Reg.	SVMs	Simple NN	CNN
Train Accuracy	92.38	96.46	92.88	95.66
Test Accuracy	92.06	92.21	92.06	92.64

Table 2: Scene 1 Mono-Temporal Results

	Softmax Reg.	SVMs	Simple NN	CNN
Train Accuracy	81.63	86.43	86.72	87.56
Test Accuracy	81.56	85.79	85.96	86.01

Table 3: Scene 2 Multi-Temporal Results

	Softmax Reg.	SVMs	Simple NN	CNN
Train Accuracy	76.21	85.78	81.74	87.14
Test Accuracy	76.05	81.07	81.43	85.50

Table 4: Scene 2 Mono-Temporal Results

	Softmax Reg.	SVMs	Simple NN	CNN
Train Accuracy	47.23	53.39	48.52	57.22
Test Accuracy	45.26	49.93	45.87	53.65

Confusion matrices are shown in Figures 4 and 5 for the CNN classifier, which performed the best in all cases. A visualization of the crop classification on a subregion of Scene 2 can be scene in Fig. 6.

Figure 4: Confusion matrices for the CNN classification results of Scene 1 in both multi- and mono-temporal cases. The y axis of the confusion matrices correspond to true labels, while the x axis corresponds to predicted labels.

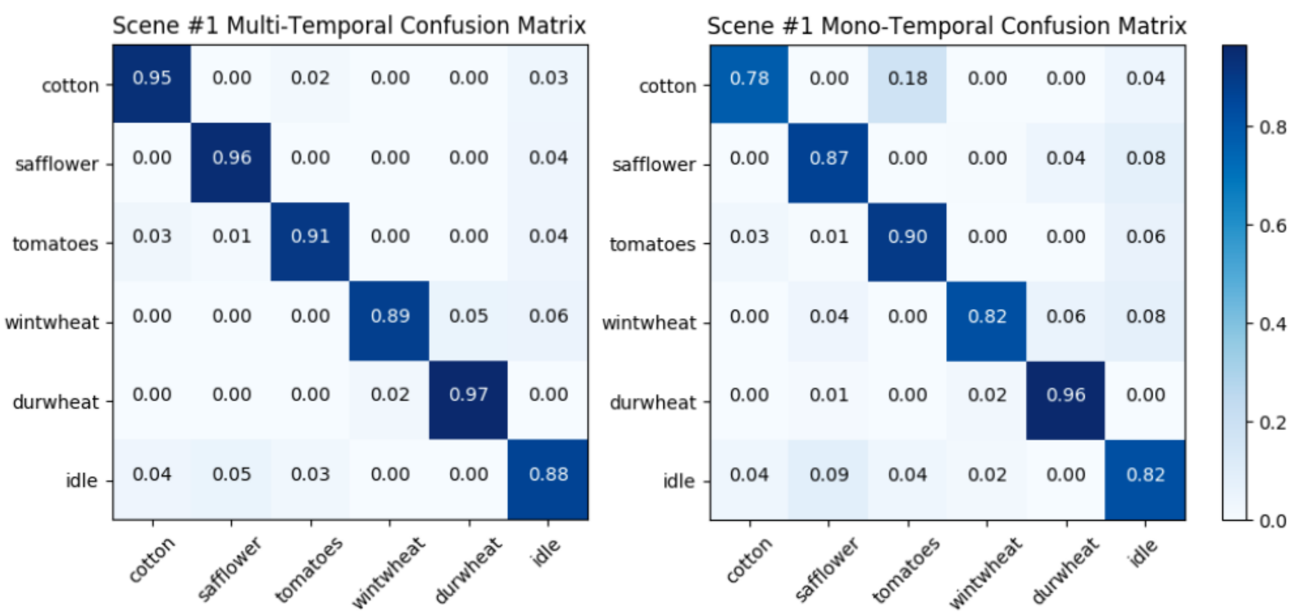

5 Conclusions

A comparison of mono- vs. multi-temporal results shows that temporal information can be helpful for successful crop classification. Surprisingly, all methods did well on Scene 1, with test accuracies around 92% for the multi-temporal case and 85% for the mono-temporal case. Scene 2, which has more classes and a more sporadic placement of crop types, shows lower performance for all methods. However, comparing the results in Tables 3 and 4, it is evident that temporal information is crucial for successful classification results of this more complicated scene.

6 Future Work

I see many areas to extend and improve this work. In regards to input data features, the current data points are normalized spectral irradiance values at the satellite sensor. If atmospheric correction were applied to the data, the ground reflectance

Figure 5: Confusion matrices for the CNN classification results of Scene 2 in both multi- and mono-temporal cases. The y axis of the confusion matrices correspond to true labels, while the x axis corresponds to predicted labels.

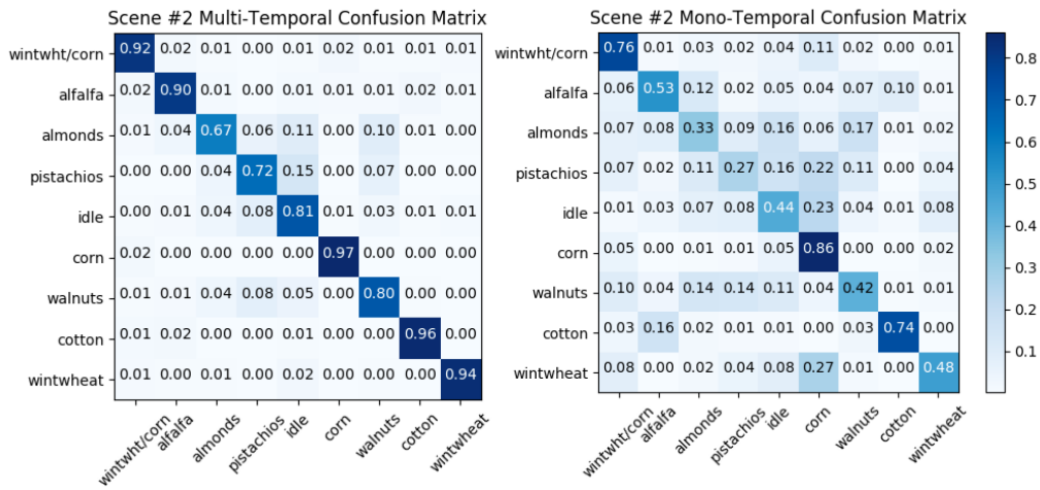

Figure 6: A qualitative visual result of the crop classification in an arbitrary region selected from Scene 2. The left image shows the ground truth labels of the crops from the USDA database, while the right image shows the predicted labels from the CNN model. The resolution is clearly finer in the predicted labels, which is expected since the Rapid Eye data has 5m resolution (compared to the 30m resolution of the ground truth).

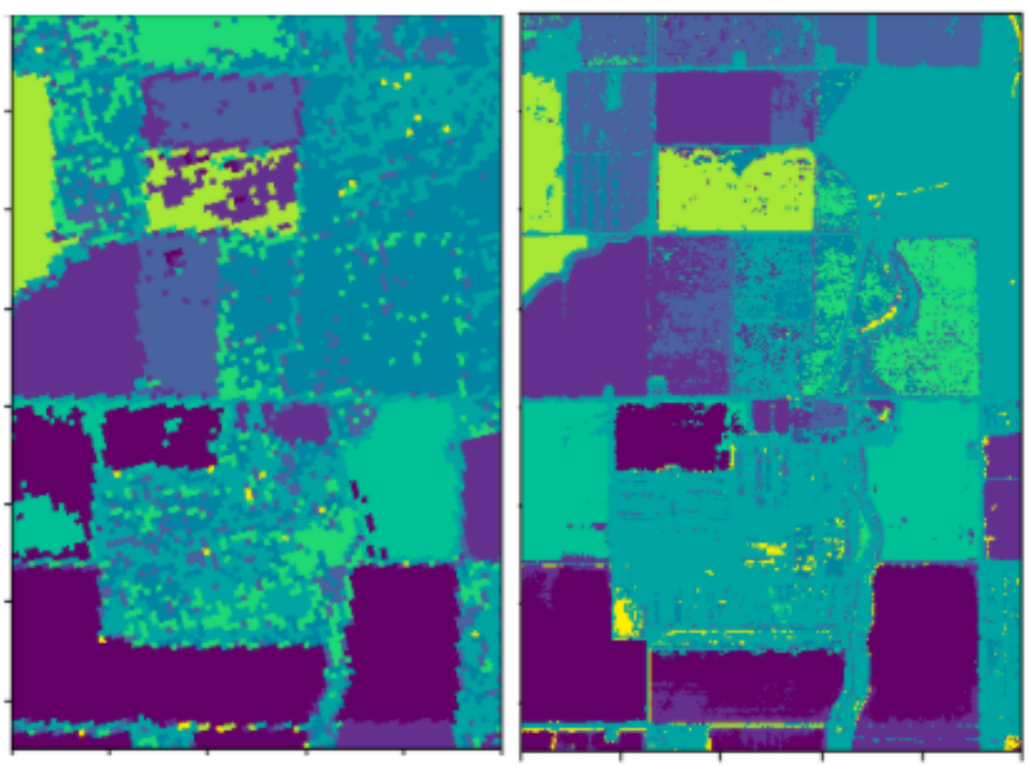

values would be invariant to illumination changes. This would yield more stable and consistent input features for training, which would also allow the model to generalize to other regions, regardless of illumination fluctuations. Textural features (such as from local binary patterns (LBP) or the gray level co-occurence matrix) may provide helpful spatial information from pixels in local neighborhoods. Incorporation of spatial information will likely boost performance.

I would like to continue this work using Planet data from 2017 for a similar analysis once the USDA Crop Data Layer is released for the year. The current cadence of Planet satellites is near daily, providing even richer temporal information compared to what was used in this project with 2016 data (approximately one image per month). It would be interesting to investigate the performance of LSTMs on the temporal dataset, as well as semantic segmentation methods that take the entire image as input.

7 Acknowledgments

I would like to thank Professor Andrew Ng and Professor Dan Boneh for a fantastic class in machine learning. I would also like to thank Kat Scott and the Image Analytics team at Planet Labs, who have provided guidance throughout this project and have introduced me to Planet's amazing set of global imagery.

8 Contributions

The project was completed by one student. Therefore, all contributions of work for this project has been completed by the author.

References

[1] Foerster, S. & Kaden, K. & Forster, M. & Itzerott, S. (2012) Crop type mapping using spectral-temporal profiles and phenological information, *Computers and Electronics in Agriculture, 89*, pp. 30–40.

[2] Peña, J., Gutierrez, P., Hervas-Martinez, C., Six, J., Plant, R., & Lopez-Granados, F. (2014) Object-Based Image Classification of Summer Crops with Machine Learning Methods *Remote Sensing, 6*; doi:10.3390/rs6065019, pp. 5019–5041.

[3] Tripathi, M., & Maktedar, D. (2016). Recent machine learning based approaches for disease detection and classification of agricultural products *IEEE International Conference on Computing Communication Control and Automation (ICCUBEA)*; doi:10.1109/ICCUBEA.2016.7860043

[4] Mishra, S., Mishra, D., & Harri, S. (2016). Applications of Machine Learning Techniques in Agricultural Crop Production: A Review Paper. *Indian Journal of Science and Technology, 9*; doi:10.17485/ijst/2016/v9i38/95032

[5] Rubwurm, M. & Korner, M. (2017) Multi-temporal land cover classification with long short-term memory neural networks *The International Archives of Photogrammetry, Remote Sensing, and Spatial Information Sciences (ISPRS), XLII-1/W1*, pp. 551–558.

[6] Planet Explorer Beta, *Planet Labs*, https://www.planet.com/explorer/

[7] CropScape - Crop Data Layer, *United States Department of Agriculture, National Agriculture Statistics Service*, https://nassgeodata.gmu.edu/CropScape/

[8] Scikit learn, sklearn.linear_model.LogisticRegression, http://scikit-learn.org/stable/modules/generated/sklearn.linear_model.LogisticRegression.html

[9] Scikit learn, *Support Vector Machines*, http://scikit-learn.org/stable/modules/svm.html

[10] Keras, Getting started with the Keras Sequential model, *Keras Documentation*, https://keras.io/getting-started/sequential-model-guide/

[11] Glorot, X., & Bengio, Y. (2010). Understanding the difficulty of training deep feedforward neural networks, *Proceedings of the Thirteenth International Conference on Artificial Intelligence and Statistics, PLMR*, 9: pp. 249–256.

[12] Zeiler, M. (2012). ADADELTA: An Adaptive Learning Rate Method, *arXiv:1212.5701*

[13] Kingma, D. P., & Ba, J. (2015). Adam: A method for Stochastic Optimization, *3rd International Conference for Learning Representations*, San Diego